International Journal of Nanoscience
Vol. 2, No. 6 (2003) 527–534

World Scientific
www.worldscientific.com

CURRENT INDUCED ENTANGLEMENT OF DOUBLE QUANTUM DOT EXCITONS

YUEH-NAN CHEN* and DER-SAN CHUU
Department of Electrophysics, National Chiao-Tung University
Hsinchu 300, Taiwan
**ynchen.ep87g@nctu.edu.tw*

We propose to measure Purcell effect by observing the current through a semeiconductor quantum dot embedded inside a microcavity. The stationary current is shown to be altered if one varies the cavity length. For the double-dot system, we find that the stationary current shows oscillatory behavior as one varies the inter-dot distance. Furthermore, the current is suppressed if the dot distance is small compared to the wavelength of the emitted photon. This photon trapping phenomenon generates the entangled state and may be used to control the emission of single photons at predetermined times.

Keywords: Exciton; quantum dot; entanglement.

1. Introduction

Historically, the idea of controlling the SE rate by using a cavity was introduced by Purcell.[1] Considering the interaction between the atomic dipole and the electromagnetic fields inside a cavity, the SE rate can be expressed as $(2\pi/\hbar)\ \rho_{\rm cav}(\omega)|\langle f|V|i\rangle|^2$, where $\rho_{\rm cav}(\omega)$ and V are the photon density of states and atom–vacuum field interaction Hamiltonian, respectively. For a planar cavity with distance L_c between two mirrors, the photon density of states is $N_c\omega/2\pi c^2$, where N_c is an integer less than $2L_c/\lambda$. Thus, by varying the cavity length L_c, the SE rate can be altered. The enhanced and inhibited SE rate for the atomic system was intensively investigated in the 1980s[2–5] by using atoms passed through a cavity. Turning to semiconductor systems, the electron–hole pair is naturally a candidate for examining the spontaneous emission. Experimentalists are now able to fabricate the quantum dot systems in laterally-structured microcavities that exhibit photon confinement in all three dimensions. Both inhibition and enhancement of the spontaneous emission of the quantum dot excitons have been observed.[6]

On the other hand, great attention has been focused on the entanglement issue since the generation of highly-entangled states is one of the fundamental requirements for quantum information processing.[7] Many previous works have been associated with quantum-optic and atomic systems.[8] However, due to the scalability of the quantum processor, solid-state realizations of such phenomena are the favored

choices.[9] In fact, super-radiance effect can also generate entanglement by spontaneous emission. Therefore, a different way is proposed to observe Purcell effect and generate the entangled states in this work. By injecting electrons and holes into the quantum dots embedded inside a microcavity, photons are generated by the recombination of the excitons. This process not only allows one to determine Purcell effect by measuring the stationary current, but also induces the entangled states in quantum dot systems.

2. Current Through One Quantum Dot and Purcell Effect

We first consider a quantum dot embedded in a *p–i–n* junction, which is similar to the device proposed by O. Benson *et al.*[10] Both the hole and electron reservoirs are assumed to be in thermal equilibrium. After a hole is injected into the hole subband in the quantum dot, the *n*-side electron can tunnel into the exciton level because of the Coulomb interaction between the electron and hole. Thus, we may assume three dot states

$$|0\rangle = |0,h\rangle\,, \qquad |U\rangle = |e,h\rangle\,, \qquad \text{and} \qquad |D\rangle = |0,0\rangle\,, \tag{1}$$

where $|0,h\rangle$ means there is one hole in the quantum dot, $|e,h\rangle$ is the exciton state, and $|0,0\rangle$ represents the ground state with no hole and electron in the quantum dot. One might argue that one cannot neglect the state $|e,0\rangle$ for real device since the tunable variable is the applied voltage. This can be resolved by fabricating a thicker barrier on the electron side so that there is little chance for an electron to tunnel in advance. Moreover, the charged exciton and biexcitons states are also neglected in our calculations. This means a low injection limit is required in the experiment.[11] We can now define the dot-operators $\hat{n}_U \equiv |U\rangle\langle U|$, $\hat{n}_D \equiv |D\rangle\langle D|$, $\hat{p} \equiv |U\rangle\langle D|$, $\hat{s}_U \equiv |0\rangle\langle U|$, and $\hat{s}_D \equiv |0\rangle\langle D|$. The total Hamiltonian H of the system consists of three parts: the dot Hamiltonian, the photon bath, and the electron (hole) reservoirs:

$$\begin{aligned}
H &= H_0 + H_T + H_V\,,\\
H_0 &= \varepsilon_U \hat{n}_U + \varepsilon_D \hat{n}_D + H_p + H_{\rm res}\,,\\
H_T &= \sum_k g(D_k b_k^\dagger \hat{p} + D_k^* b_k \hat{p}^\dagger) = g(\hat{p}X + \hat{p}^\dagger X^\dagger)\,,\\
H_p &= \sum_k \omega_k b_k^\dagger b_k\,,\\
H_V &= \sum_{\mathbf{q}} (V_{\mathbf{q}} c_{\mathbf{q}}^\dagger \hat{s}_U + W_{\mathbf{q}} d_{\mathbf{q}}^\dagger \hat{s}_D + \text{c.c.})\,,\\
H_{\rm res} &= \sum_{\mathbf{q}} \varepsilon_{\mathbf{q}}^U c_{\mathbf{q}}^\dagger c_{\mathbf{q}} + \sum_{\mathbf{q}} \varepsilon_{\mathbf{q}}^D d_{\mathbf{q}}^\dagger d_{\mathbf{q}}\,.
\end{aligned} \tag{2}$$

In above equations, b_k is the photon operator, gD_k is the dipole coupling strength, $X = \sum_k D_k b_k^\dagger$, and $c_{\mathbf{q}}$ and $d_{\mathbf{q}}$ denote the electron operators in the left and right

reservoirs, respectively. Here, g is a constant with a unit of the tunneling rate. The couplings to the electron and hole reservoirs are given by the standard tunnel Hamiltonian H_V, where $V_{\mathbf{q}}$ and $W_{\mathbf{q}}$ couple the channels $\mathbf{q}$ of the electron and the hole reservoirs. If the couplings to the electron and the hole reservoirs are weak, then it is reasonable to assume that the standard Born–Markov approximation with respect to these couplings is valid. In this case, one can derive a master equation from the exact time-evolution of the system. The equations of motion can be expressed as

$$\begin{aligned}
\langle\hat{n}_U\rangle_t - \langle\hat{n}_U\rangle_0 &= -ig\int_0^t dt'\{\langle\hat{p}\rangle_{t'} - \langle\hat{p}^\dagger\rangle_{t'}\} + 2\Gamma_U\int_0^t dt'(1 - \langle\hat{n}_U\rangle_{t'} - \langle\hat{n}_D\rangle_{t'})\,,\\
\langle\hat{n}_D\rangle_t - \langle\hat{n}_D\rangle_0 &= -ig\int_0^t dt'\{\langle\hat{p}\rangle_{t'} - \langle\hat{p}^\dagger\rangle_{t'}\} - 2\Gamma_D\int_0^t dt'\langle\hat{n}_D\rangle_{t'}\,,\\
\langle\hat{p}\rangle_t - \langle\hat{p}\rangle_t^0 &= -\Gamma_D\int_0^t dt' e^{i\varepsilon(t-t')}\langle X_t X_{t'}^\dagger\tilde{p}(t')\rangle_{t'}\\
&\quad - ig\int_0^t dt' e^{i\varepsilon(t-t')}\{\langle\hat{n}_U X_t X_{t'}^\dagger\rangle_{t'} - \langle\hat{n}_D X_{t'}^\dagger X_t\rangle_{t'}\}\,,\\
\langle\hat{p}^\dagger\rangle_t - \langle\hat{p}\rangle_t^0 &= -\Gamma_D\int_0^t dt' e^{-i\varepsilon(t-t')}\langle\tilde{p}^\dagger(t')X_{t'}X_t^\dagger\rangle_{t'}\\
&\quad + ig\int_0^t dt' e^{-i\varepsilon(t-t')}\{\langle\hat{n}_U X_{t'}X_t^\dagger\rangle_{t'} - \langle\hat{n}_D X_t^\dagger X_{t'}\rangle_{t'}\}\,.
\end{aligned} \tag{3}$$

where $\Gamma_U = \pi\sum_{\mathbf{q}} V_{\mathbf{q}}^2\delta(\varepsilon_U - \varepsilon_{\mathbf{q}}^U)$, $\Gamma_D = \pi\sum_{\mathbf{q}} W_{\mathbf{q}}^2\delta(\varepsilon_D - \varepsilon_{\mathbf{q}}^D)$, and $\varepsilon = \varepsilon_U - \varepsilon_D$ is the energy gap of the quantum dot exciton. Here, $\tilde{p}(t') = pe^{i\varepsilon t}X_{t'}$, and $X_{t'}$ denotes the time evolution of X with H_p. The expectation value $\langle\hat{p}^{(\dagger)}\rangle_t^0$ describes the decay of an initial polarization of the system and plays no role for the stationary current. Therefore, we shall assume the initial expectation value of $\hat{p}^{(\dagger)}$ vanishes at time $t = 0$.

As can be seen from Eq. (3), there are terms like $\langle\hat{n}_U X_t X_{t'}^\dagger\rangle_{t'}$ which contain products of dot operators and photon operators. If we are interested in small coupling parameters, a decoupling of the reduced density matrix $\tilde{\rho}(t')$ can be written as $\tilde{\rho}(t') \approx \rho_{ph}^0\mathrm{Tr}_{ph}\tilde{\rho}(t')$. By using the above equations, we obtain $\mathrm{Tr}(\tilde{\rho}(t')\hat{n}_U X_t X_{t'}^\dagger) \approx \langle\hat{n}_U\rangle_{t'}\langle X_t X_{t'}^\dagger\rangle_0$ and correspondingly the other products of operators can be also obtained. For spontaneous emission, the photon bath is assumed to be in equilibrium. The expectation value $\langle X_t X_{t'}^\dagger\rangle_0 \equiv C(t-t')$ is a function of the time interval only. We can now define the Laplace transformation for real z,

$$C_\varepsilon(z) \equiv \int_0^\infty dt e^{-zt}e^{i\varepsilon t}C(t)\,, \tag{4}$$

$$n_U(z) \equiv \int_0^\infty dt e^{-zt}\langle\hat{n}_U\rangle_t\,, \quad \text{etc.}\,, \quad z > 0\,, \tag{5}$$

and transform the whole equations of motion into z-space. These equations can then be algebraically solved. The tunnel current $\hat{I}$ can be defined as the change of

the occupation of $\hat{n}_U$ and is given by $\hat{I} \equiv ig(\hat{p} - \hat{p}^\dagger)$, where we have set the electron charge $e = 1$ for convenience. The time dependence of the expectation value $\langle \hat{I} \rangle_t$ can be obtained by solving the transformed equations and performing the inverse Laplace transformation. For time $t \to \infty$, the result is

$$\langle \hat{I} \rangle_{t\to\infty} = \frac{2g^2\Gamma_U\Gamma_D B}{g^2\Gamma_D B + [g^2 B + \Gamma_D + 2\gamma\Gamma_D^2 + (\gamma^2 + \Omega^2)\Gamma_D^3]}\,, \qquad B = \gamma + (\gamma^2 + \Omega^2)\Gamma_D\,, \tag{6}$$

where $g^2\Omega$ and $g^2\gamma$ are the exciton frequency shift and decay rate, respectively.

Since the stationary current through the quantum dot depends strongly on the decay rate γ, the results of a quantum dot inside a planar microcavity is numerically displayed in Fig. 1. In plotting the figure, the current is in terms of 100 pA, and the cavity length is in units of $\lambda_0/2$, where λ_0 is the wavelength of the emitted photon. Furthermore, the tunneling rates, Γ_U and Γ_D, are assumed to be equal to $0.2\gamma_0$ and γ_0, respectively. Here, a value of 1/1.3 ns for the free-space quantum dot decay rate γ_0 is used in our calculations.[12] In addition, the planar microcavity has a Lorentzian broadening at each resonant modes (with broadening width equals to 1% of each resonant mode).[13] As the cavity length is less than half of the wavelength of the emitted photon, the stationary current is inhibited. This is because the energy of the photon generated by the quantum dot is less than the cut-off frequency of the planar microcavity. Moreover, the current is increased whenever the cavity length is equal to multiple half wavelength of the emitted photon. It represents the cavity length exceeds some multiple wavelength, opens up another decay channel abruptly for the quantum dot exciton, and turns out that the current is increased. With the increasing of cavity length, the stationary current becomes less affected by the cavity and gradually approaches free space limit.

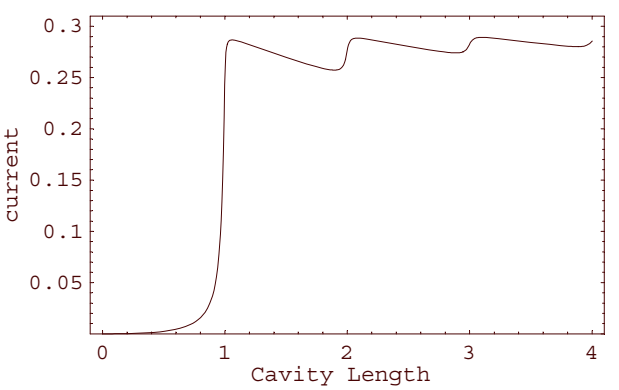

Fig. 1. Stationary tunnel current, Eq. (8), as a function of cavity length L_c. The vertical and horizontal units are 100 pA and λ_0, respectively.

3. Current Through the Double-Dot System and the Induced Entanglement

We now consider *two spatially-separated* quantum dot inside a *p–i–n* junction (Fig. 2). One of the obstacles in measuring super-radiance between the quantum dots comes from the random size of the dots which result in a random distribution of energy gap and thus diminishes the coherent radiation. This can be overcome by constructing a gate voltage over one of the quantum dots. The energy gap and the orientation of the dipole moments of one of the quantum dots, can be well controlled. In our calculation, we neglect the Forster process which may have some influences on the results if the two dots are close to each other. The validity of this assumption will be discussed later.

Thus, we may assume four dot states $|0\rangle = |0, h; 0, 0\rangle$, $|U_1\rangle = |e, h; 0, 0\rangle$, $|U_2\rangle = |0, 0; e, h\rangle$, and $|D\rangle = |0, 0; 0, 0\rangle$, where $|0, h; 0, 0\rangle$ means there is one hole in dot 1 and $|0, 0; 0, 0\rangle$ represents the ground state with no hole and electron in the quantum dots. The exciton states $|e, h; 0, 0\rangle$ (in dot 1) can be converted to $|0, 0; e, h\rangle$ (in dot 2) through the exciton–photon interactions. By transforming $|U_1\rangle$ and $|U_2\rangle$ into Dicke states: $|S_0\rangle = (1/\sqrt{2})(|U_1\rangle - |U_2\rangle)$ and $|T_0\rangle = (1/\sqrt{2})(|U_1\rangle + |U_2\rangle)$, we can now define the dot-operators $\hat{n}_S \equiv |S_0\rangle\langle S_0|$, $\hat{n}_T \equiv |T_0\rangle\langle T_0|$, $\hat{n}_D \equiv |D\rangle\langle D|$, $\hat{p}_s \equiv |S_0\rangle\langle D|$, $\hat{p}_T \equiv |T_0\rangle\langle D|$, $\hat{s}_{U_1} \equiv (1/\sqrt{2})(|0\rangle\langle S_0| + |0\rangle\langle T_0|)$, $\hat{s}_D \equiv |0\rangle\langle D|$. Similar to the one-dot case, one can derive the stationary tunnel current through the double-dot system:

$$\langle \hat{I} \rangle_{t\to\infty} = \frac{4g^2\gamma_+\gamma_-}{\gamma_- + \gamma_+[1 + 2\gamma_-(g^2/\Gamma_D + g^2/\Gamma_U + \Gamma_D)]}\,, \tag{7}$$

where $g^2\gamma_+$ and $g^2\gamma_-$ are the super-radiant and sub-radiant decay rate of the exciton, respectively.[14] The corresponding decay rate for super-radiant and the sub-radiant channels is given by

$$g^2\gamma_\pm = \gamma_0 \left(1 \pm \frac{\sin(2\pi d/\lambda_0)}{2\pi d/\lambda_0}\right), \tag{8}$$

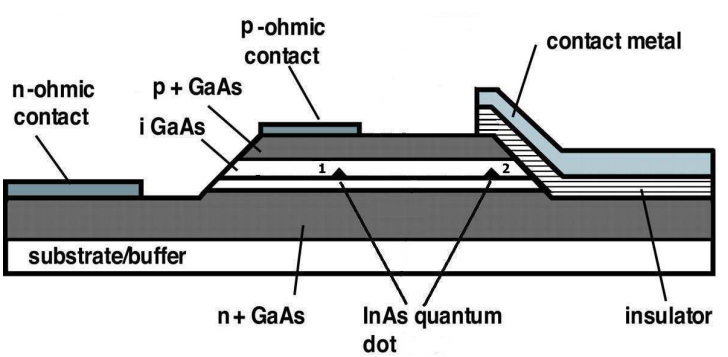

Fig. 2. Two InAs quantum dots are embedded in a *p–i–n* junction. Above dot 2 is a metal gate, which control the energy gap and the orientation of the dipole.

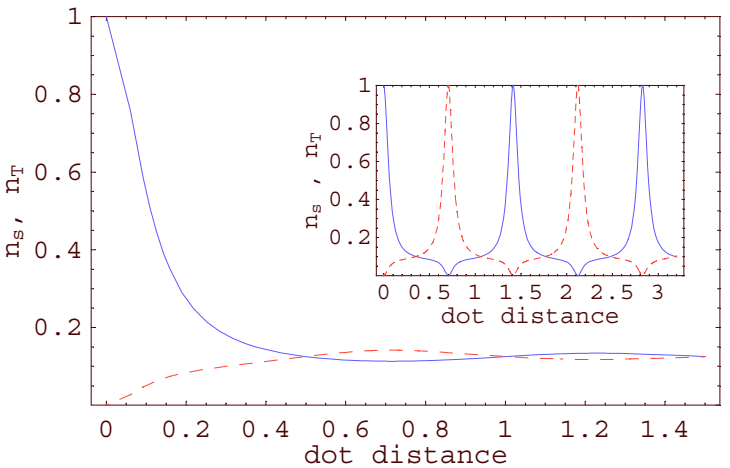

Fig. 3. Occupation probability of the entangled states n_S (—) and n_T (- - -). The inset shows the results inside a rectangular microcavity. The horizontal unit used here is λ_0.

where d is the inter-dot distance and γ_0 is the exciton decay rate in a quantum dot. As can be seen from Eq. (6), the current is suppressed as the dot distance d is much smaller than the wavelength of the emitted photon. This corresponds to the trapping state in the two-ion system. As long as we choose only one of the dots to be coupled to reservoirs, the generated photon is reabsorbed immediately by the other dot and vice versa. The current is then blocked by this exchange process. Similar to the two-ion super-radiance, the current also exhibits oscillatory behavior as a function of dot distance.

In Fig. 3, we plot the expectation value of $\hat{n}_S$ ($\hat{n}_T$) as a function of the dot distance. The maximum entangled state ($|S_0\rangle$) is reached as $d \ll \lambda_0$. This is remarkable as the steady state is independent of the initial state. The entanglement is induced by the cooperative decoherence in the system. In a recent paper by Schneider and Milburn,[15] the authors considered the behavior of an ion trap with all ions driven simultaneously and coupled collectively to a heat bath. They also found that the steady state of the ion trap can exhibit quantum entanglement. However, the concurrence of their system is below the value of unity (maximum entanglement). On the contrary, in our system the maximum entangled state can be generated by tuning the band gap of dot 2 (linear stark effect), i.e., control the on/off of the super-radiance. Another advantage of our scheme is shown in the inset of Fig. 3. If the double-dot system is incorporated inside a *rectangular microcavity*, the maximum entangled states repeat as a function of inter-dot distance. This means that even for remote separation, the entanglement can still be achieved. The reason can be attributed to the creation of entanglement in our model that is governed by the interaction with a common heat bath, while conventional creation of entanglement depends on the direct interaction between two subsystems.[16] When two dots are coupled to the common photon fields, the collective decay process drives the

system into the entangled states. The novel feature of the effect predicted here is that entanglement in fact can be controlled electrically (without applying a laser field) and read out in the form of a transport property, i.e., the electron *current* (as a function of the dot distance or, alternatively, the cavity length).

Another possible application of this effect is that by tuning the coherence of the dots, one can control the emission of single photon at predetermined times, which is important for the field of quantum information technology. One might argue that for small inter-dot distance the Forster process may play some role in our system[17]; nevertheless, this only causes small energy splitting between state $|S_0\rangle$ and $|T_0\rangle$. Comparing to the large energy difference in the III–V semiconductor material, its effect on the decay rate $g^2\gamma_\pm$ is negligible. As for the problem of dissipation, decoherence due to interaction with other bosonic excitations (phonons and electron–hole pairs in the leads) is inevitable but can in principle be (partly) controlled by variation of the dot energies, or control of the mechanical degree of freedom.[18] In addition, scattering due to impurities are negligible since there is no inter-dot transport in our system.

4. Summary

In conclusion, we have proposed a method of detecting Purcell effect in a semiconductor quantum dot system. By incorporating the InAs quantum dot between a *p–i–n* junction surrounded by a planar microcavity, the Purcell effect on stationary tunnel current can be examined by changing the cavity length. For the double-dot system, the super-radiant effect can also be observed by measuring the stationary current. The maximum entangled state is induced as the inter-dot distance is much smaller than the wavelength of the emitted photon. Our model provides a new way to generate the entanglement in solid-state systems.

References

1. E. M. Purcell, *Phys. Rev.* **69**, 681 (1946).
2. P. Goy, J. M. Raimond, M. Gross, and S. Haroche, *Phys. Rev. Lett.* **50**, 1903 (1983).
3. G. Gabrielse and H. Dehmelt, *Phys. Rev. Lett.* **55**, 67 (1985).
4. R. G. Hulet, E. S. Hilfer and D. Kleppner, *Phys. Rev. Lett.* **55**, 2137 (1985).
5. D. J. Heinzen, J. J. Childs, J. E. Thomas, and M. S. Feld, *Phys. Rev. Lett.* **58**, 1320 (1987).
6. M. Bayer, T. L. Reinecke, F. Weidner, A. Larionov, A. McDonald, and A. Forchel, *Phys. Rev. Lett.* **86**, 3168 (2001).
7. C. H. Bennett and D. P. DiVincenzo, *Nature* (*London*) **404**, 247 (2000).
8. T. Pellizzari, S. A. Gardiner, J. I. Cirac, and P. Zoller, *Phys. Rev. Lett.* **75**, 3788 (1995); J. I. Cirac and P. Zoller, *Phys. Rev. Lett.* **74**, 4091 (1995); K. Molmer and A. Sorensen, *Phys. Rev. Lett.* **82**, 1835 (1999).
9. A. T. Costa, Jr. and S. Bose, *Phys. Rev. Lett.* **87**, 277901 (2001); W. D. Oliver, F. Yamaguchi and Y. Yamamoto, *Phys. Rev. Lett.* **88**, 037901 (2002); O. Gywat, G. Burkard and D. Loss, *Phys. Rev. B* **65**, 205329 (2002).
10. O. Benson, C. Santori, M. Pelton, and Y. Yamamoto, *Phys. Rev. Lett.* **84**, 2513 (2000).

11. Z. Yuan, B. E. Kardynal, R. M. Stevenson, A. J. Shields, C. J. Lobo, K. Cooper, N. S. Beattie, D. A. Ritchie, and M. Pepper, *Science* **295**, 102 (2002).
12. G. S. Solomon, M. Pelton and Y. Yamamoto, *Phys. Rev. Lett.* **86**, 3903 (2001).
13. Y. N. Chen, D. S. Chuu, T. Brandes, and B. Kramer, *Phys. Rev. B* **64**, 125307 (2001).
14. P. S. Lee, Y. C. Lee and C. T. Chang, *Phys. Rev. A* **8**, 1722 (1973).
15. S. Schneider and G. J. Milburn, *Phys. Rev. A* **65**, 042107 (2002).
16. D. Braun, *Phys. Rev. Lett.* **89**, 277901 (2002).
17. L. Quiroga and N. Johnson, *Phys. Rev. Lett.* **83**, 2270 (1999).
18. S. Debald, T. Brandes and B. Kramer, *Phys. Rev. B* **66**, 041301 (2002).